Proceedings of the 17th Czech and Slovak Conference on Magnetism, Košice, Slovakia, June 3–7, 2019

# Magnetic Resonance Contrast Imaging of Ferritin and Magnetoferritin at 7 T

M. Mihalikova[a,*], L. Balejcikova[b], P. Kopcansky[c], D. Dobrota[a] and O. Strbak[d]

[a]Department of Medical Biochemistry, Jessenius Faculty of Medicine in Martin, Comenius University in Bratislava, Mala Hora 4, 036 01 Martin, Slovakia

[b]Institute of Hydrology, Slovak Academy of Sciences, Dubravska cesta 9, 841 04 Bratislava, Slovakia

[c]Institute of Experimental Physics, Slovak Academy of Sciences, Watsonova 47, 040 01 Kosice, Slovakia

[d]Biomedical Center Martin, Jessenius Faculty of Medicine in Martin, Comenius University in Bratislava, Mala Hora 4, 036 01 Martin, Slovakia

We studied the relaxation properties of native (physiological) ferritin and magnetoferritin (as a model system of pathological ferritin) in order to develop a magnetic resonance imaging methodology for the contrast imaging and differentiation of physiological and pathological ferritin in high-field MRI systems. MRI measurements were performed using a 7 T system using longitudinal $T_1$ and transverse $T_2$ relaxation time mapping protocols. The relative contrast and relaxation time of native ferritin and magnetoferritin with different loading factors were analysed and compared. The results clearly show a significant difference between native ferritin and magnetoferritin in $T_2$-weighted protocols. The difference in the $T_1$-weighted protocol is also obvious but not as significant as in the $T_2$-weighted protocols. These results reflect the different iron mineral core compositions of native ferritin and magnetoferritin. Our findings could significantly contribute to the exploitation of iron oxide accumulation in non-invasive diagnostics of pathological processes related to disrupted iron homeostasis (e.g., neurodegenerative disorders).

DOI: 10.12693/APhysPolA.137.650

PACS/topics: magnetic resonance imaging, magnetoferritin, ferritin, relaxation time, contrast

## 1. Introduction

Iron is an essential nutrient for almost all living cells [1]. In the form of ferrous ($Fe^{2+}$) or ferric ($Fe^{3+}$) ions, iron is usually incorporated into the protein structure. Ferric ions are non-toxic to cells, while ferrous ions produce hydroxyl radicals through the Fenton reaction [1]. This represents oxidative stress for the cell. Therefore, cells and organisms have developed the ability to eliminate the toxicity of ferrous ions. One of the mechanisms used by all biological systems is ferritin [2]. Ferritin particles are designed to transport and convert highly toxic ferrous ions into ferric ions inside the hollow ferritin envelope. The mineral core of the physiological native ferritin (NF) consists of ferrihydrite-like crystal. However, a recent study confirmed the presence of magnetite-like structures in the brain of a patient with Alzheimer's disease compared to healthy brain tissue [3]. It is believed that the precursor of their formation is a ferrihydrite core in ferritin, which transforms to magnetite due to impaired iron homeostasis [4]. Such pathological ferritin particles have a permanent magnetic moment, so they can be modeled by magnetoferritin, which consists of a protein envelope and magnetite crystal [5]. Currently, a clinical, non-invasive methodology able to distinguish physiological and pathological ferritin does not exist. Therefore, the main goal of our study is to provide, with the help of magnetoferritin as a pathological ferritin model system, a measurement protocol that enables non-invasive and clear contrast differentiation of physiological and pathological ferritin in high-field MRI systems.

## 2. Materials and methods

Magnetoferritin was prepared by the incorporation of ferrous ions into the empty protein shell of native apoferritin by the synthesis method described in [5]. Several types of magnetoferritin samples with different loading factors (LFs), representing the average number of iron atoms per apoferritin, were prepared: MF1 (LF = 553), MF2 (LF = 733), MF3 (LF = 872). The LF of NF is 884.

MRI measurements were performed using a 7 T BioSpec Bruker system. Before the measurements, the magnetoferritin and NF were diluted to a concentration gradient of iron oxide of $2.5 \times 10^{-3}$, $5 \times 10^{-3}$, $7.5 \times 10^{-3}$, 0.01, 0.0125, 0.015, 0.0175, or 0.02 mg/ml. The measurements were carried out for the samples of NF, MF1, MF2, and MF3.

To determine the most suitable protocol for the comparative imaging of NF and magnetoferritin, two different ($T_1$ and $T_2$ parametric mapping) pulse sequences, with different measurement protocols were used:

*corresponding author; e-mail: martinamihalikova09@gmail.com

- $T_1$ mapping rapid acquisition with refocused echoes (RARE) pulse sequence;
- $T_2$ mapping multi-slice multi-echo (MSME) pulse sequence.

The relative contrast and longitudinal and transversal relaxation times were analysed and compared. The relative contrast RC of iron oxide as a negative contrast agent ($I_0 > I$) is defined as follows [5]:

$$\mathrm{RC} = (I - I_0)/I_0, \tag{1}$$

where $I_0$ is the intensity without magnetite particles and $I$ represents the signal intensity with magnetite nanoparticles.

Subsequently, the longitudinal and transversal relaxation times ($T_1$ and $T_2$) of the samples were determined by fitting with the following functions:

$$M(t) = A + M_0(1 - \exp(t/T_1)), \tag{2}$$

$$y = A + C\exp(-t/T_2), \tag{3}$$

where $M_0$ is the equilibrium magnetization, $A$ is the absolute bias, $t$ is the time, $T_1$ is the longitudinal recovery time, $C$ is the signal intensity, and $T_2$ is the transversal relaxation time.

Equation (2) characterizes the return of the magnetic moment to the equilibrium and is dependent on the spin–lattice interaction with a transfer of energy. On the other hand, Eq. (3) describes transversal magnetization decrease due to the spin–spin interactions, with no transfer of energy.

The Paravision "Image Sequence Analysis" tool (Bruker, Germany) and OriginPro2019 (Originlab Corporation, Wellesley Hills, USA) were used for data processing.

## 3. Results

The NF and MF samples were measured with $T_1$ and $T_2$ mapping pulse sequences (RARE and MSME) to obtain the signal intensity ($I_0$ and $I$) and the relaxation time ($T_1$ and $T_2$) values at 7 T. We sought to determine the most suitable protocol for comparative imaging of NF and magnetoferritin. The main goal was to find out whether the magnetoferritin, as a pathological model system of iron accumulation, can be clearly distinguished from NF by comparison of the relative contrast and relaxation times. The following protocols were established as the most efficient in contrast imaging of our samples:

- $T_1$ mapping RARE pulse sequence, with repetition time TR = 5500, 3000, 1500, 800, 400, and 200 ms, and echo time TE= 7 ms;
- $T_2$ mapping MSME pulse sequence, with repetition time TR = 2000 ms, starting echo time TE = 8 ms, spacing = 8 ms, and 25 images.

The relaxation time $T_1$ of samples acquired with the $T_1$ mapping RARE pulse sequence is shown in Fig. 1a. We observe a decrease in $T_1$ with increasing concentration of iron oxide. The only exception is the lowest concentration (2.5 $\mu$g/ml) (Fig. 1a), where the increase in relaxation time $T_1$ is observed, behaving as a positive contrast agent. However, in general, magnetoferritin shortens the relaxation time $T_1$ compared to ferritin (Fig. 1a, c).

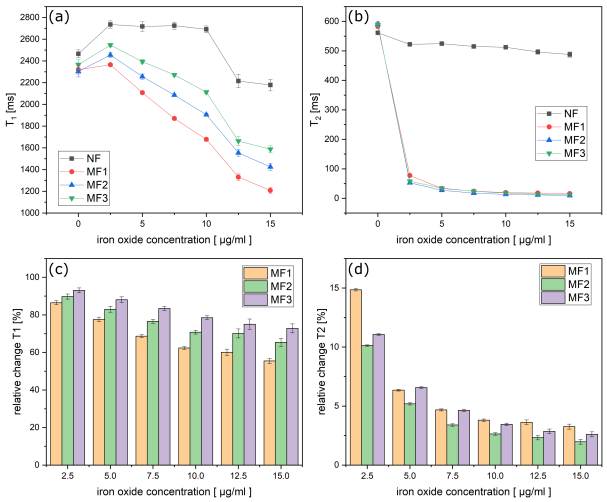


Fig. 1. Comparison of NF and magnetoferritin: (a) relaxation time $T_1$ depending on concentration, (b) relaxation time $T_2$ depending on concentration, (c) relative change in relaxation time $T_1$ of magnetoferritin versus NF (100%), (d) relative change in relaxation time $T_2$ of magnetoferritin versus NF (100%).

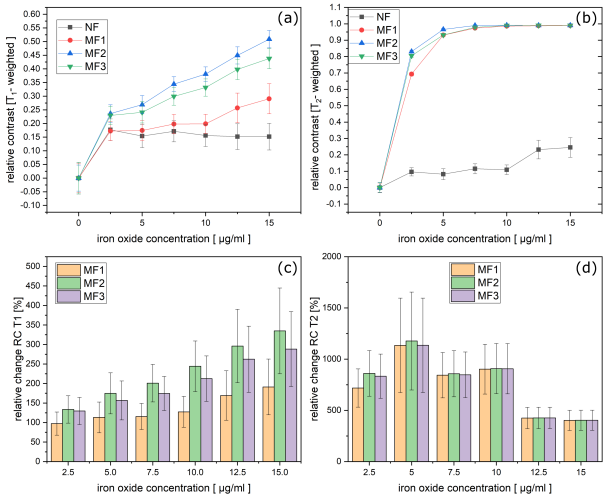


Fig. 2. Relative contrast of NF and magnetoferritin: (a) relative contrast of magnetoferritin (MF1, MF2 and MF3) in comparison with NF with data obtained by the $T_1$ mapping RARE pulse sequence, (b) relative contrast of magnetoferritin (MF1, MF2 and MF3) in comparison with NF. Data were obtained by the $T_2$ weighted MSME pulse sequence, (c) comparison of relative change of the $T_1$-weighted relative contrast of magnetoferritin compared to NF (100%), (d) comparison of relative change of the $T_2$-weighted relative contrast of magnetoferritin compared to NF (100%).

Figure 1b describes the relaxation time $T_2$ acquired with the $T_2$ mapping MSME pulse sequence. The relaxation time $T_2$ of all MF samples significantly decreases with an increasing concentration of iron oxide. The difference between NF and MF is clearly visible in the $T_2$ plot (Fig. 1b), as well as in the relative change plot (NF = 100%), where the change ranges from a 2 to 15% increase (Fig. 1d).

Figure 2a shows the relative contrast decrease caused by the $T_1$ mapping RARE pulse sequence. The relative contrast change (NF = 100%) of MF samples ranges from $\approx$ 100 to 330% in comparison with NF (Fig. 2c). Figure 2b describes the significant contrast change caused by the $T_2$ mapping MSME pulse sequence. It is accompanied by the sharp shortening of the transversal relaxation time $T_2$ (Fig. 1b) in comparison with the longitudinal relaxation time $T_1$ (Fig. 1a).

## 4. Discussion

Currently, biological iron imaging is highly sought after in clinical practice since a significant number of pathological processes are associated with iron oxide nanoparticle accumulation. However, a clinically usable methodology is still missing. The crucial point is to establish imaging parameters that allow a reproducible and clear differentiation of physiological and pathological iron. We focused on the $T_1$ and $T_2$ mapping pulse sequences that are widespread in clinical practice and have relatively short time of signal acquisition. We found that all magnetoferritin samples shorten both the $T_1$ and $T_2$ relaxation times. However, as can be seen in Fig. 1, the decrease in $T_2$ time is considerably larger. This indicates that the $T_2$ relaxation mechanism prevails in magnetoferritin at 7 T, which is in accordance with previous results for lower fields [5]. The same situation as with the relaxation time, occurs with the comparison of the relative contrast acquired with both sequences, as described in Fig. 2. We observed the clear differentiation of all MF LFs and iron oxide concentrations in comparison with NF. The prevailing $T_2$ shortening must be considered during development of an MRI methodology for comparative imaging of NF and pathological ferritin. In addition, another important feature must be taken into account: a positive signal from the lowest magnetoferritin concentration, which is valid for all LFs of MF, but not for NF (Fig. 1a). The precise molecular mechanism is unknown. However, the same process was also observed in synthetically prepared magnetite nanoparticles [6].

## 5. Conclusions

The main goal of our study was to distinguish the NF and MF as a model system of pathological ferritin by standard $T_1$ and $T_2$ mapping pulse sequences at 7 T. Our data clearly show the discrimination of MF with all LFs and concentrations in comparison with NF for both sequences. However, we found the significant prevailing effect of $T_2$ relaxation in MF that was not observed in NF. These results can contribute to the development of a methodology required for non-invasive diagnosis of pathological processes associated with biogenic iron accumulation of biogenic iron.

## Acknowledgments

This work was supported by the projects: Ministry of Health (2018/11-UKMT-7), VEGA (2/0016/17, 2/0044/20), APVV (APVV-015-0453), and Competence Center Martin (ITMS code: 26220220153).

## References

[1] J. Wang, K. Pantopoulos, *Biochem. J.* **434**, 365 (2011).

[2] N.D. Chasteen, P.M. Harrison, *J. Struct. Biol.* **126**, 182 (1999).

[3] L. Bossoni, L.G. Mourse, M. Bulk, et al., *J. Phys. Condens. Matter* **29**, 415801 (2017).

[4] J. Dobson, *FEBS Lett.* **496**, 1 (2001).

[5] O. Strbak, L. Balejcikova, L. Baciak, J. Kovac, M. Masarova-Kozelova, A. Krafcik, D. Dobrota, P. Kopcansky, *J. Phys. D Appl. Phys.* **50**, 365401 (2017).

[6] I. Khmara, O. Strbak, V. Zavisova, et al., *J. Magn. Magn. Mater.* **474**, 319 (2019).